

Chiral Properties of Strong Interactions in a Magnetic Background

Francesco Negro



Unige

21 September 2011

SM&FT 2011 - Bari



INFN

In collaboration with:
Based on:

Massimo D'Elia
Phys. Rev. D 83, 114028 (2011)

Outline

- ▶ 1) L-QCD in external (background) magnetic field.
- ▶ 2) Magnetic catalysis and chiral symmetry breaking.
- ▶ 3) Numerical results and comparison with other models.
- ▶ 4) Conclusions.

1) L-QCD in external (background) magnetic field.

Why studying QCD in a magnetic background?

Theoretical point of view: B is a further direction in parameter space to probe QCD phase diagram and vacuum properties.

Phenomenological point of view: heavy ion collision experiments, CME, cosmological phase transitions, magnetars.

Our aim:

Study how vacuum (*i.e.* zero temperature) chiral properties, such as chiral condensates, depend on the external magnetic field.

Focus on the particular case of a constant and uniform z -oriented field.

1) L-QCD in external (background) magnetic field.

Existing lattice studies.

Chromo-Magnetic field:

[P. Cea and L. Cosmai, JHEP 0508, 079 (2005)],

[P. Cea, L. Cosmai and M. D'Elia, JHEP 0712, 097 (2007)]

Chiral properties and CME (Chiral Magnetic Effect):

[P. V. Buividovich et al., Phys. Rev. D 80, 054503 (2009)],

[M. Abramczyk et al., arXiv:hep-lat/0911.1348], [Buividovich et al., arXiv:hep-lat/1003.2180]

Finite temperature and phase diagram:

[D'Elia, Sanfilippo and Mukherjee; arXiv:hep-lat/1005.5365v2] ,

[G. Endrodi; talk at Lattice2011]

1) L-QCD in external (background) magnetic field.

Discretization details and numerical setup.

QCD with $N_f = 2$ mass-degenerate flavours: u and d quark.

$$q_u = +(2/3)|e| \quad q_d = -(1/3)|e|$$

Partition function for rooted staggered fermions:

$$Z = \int \mathcal{D}U \mathcal{P}[m, U, B, Q] = \int \mathcal{D}U e^{-S_G} \det M^{1/4}[m, B, q_u] \det M^{1/4}[m, B, q_d]$$

the staggered fermion matrix M in presence of the background is:

$$M_{i,j}[B, q] = \hat{m} \delta_{i,j} + \frac{1}{2} \sum_{\mu=1}^4 \eta_{i,\mu} (U'_{i,\mu}(B, q) \delta_{i,j-\hat{\mu}} - U'^{\dagger}_{i-\hat{\mu},\mu}(B, q) \delta_{i,j+\hat{\mu}})$$

where

$$U'_{i,\mu}(B, q) = u_{i,\mu}(B, q) \cdot U_{i,\mu}$$

To have $\mathbf{B} = B\hat{z}$ we choose $A_{\mu}^{\text{EM}}(\mathbf{x}) = (0, xB, 0, 0)$ so that:

$$u_{i,\mu}(B, q) = 1 \text{ unless } \mu = y \rightarrow u_{i,y}(B, q) = e^{iea^2 i_x B}$$

1) L-QCD in external (background) magnetic field.

Discretization details and numerical setup.

QCD with $N_f = 2$ mass-degenerate flavours: u and d quark.

$$q_u = +(2/3)|e| \quad q_d = -(1/3)|e|$$

Partition function for rooted staggered fermions:

$$Z = \int \mathcal{D}U \mathcal{P}[m, U, B, Q] = \int \mathcal{D}U e^{-S_G} \det M^{1/4}[m, B, q_u] \det M^{1/4}[m, B, q_d]$$

the staggered fermion matrix M in presence of the background is:

$$M_{i,j}[B, q] = \hat{m} \delta_{i,j} + \frac{1}{2} \sum_{\mu=1}^4 \eta_{i,\mu} (U'_{i,\mu}(B, q) \delta_{i,j-\hat{\mu}} - U'^{\dagger}_{i-\hat{\mu},\mu}(B, q) \delta_{i,j+\hat{\mu}})$$

where

$$U'_{i,\mu}(B, q) = u_{i,\mu}(B, q) \quad U_{i,\mu}$$

To have $\mathbf{B} = B\hat{z}$ we choose $A_{\mu}^{\text{EM}}(\mathbf{x}) = (0, xB, 0, 0)$ so that:

$$u_{i,\mu}(B, q) = 1 \text{ unless } \mu = y \rightarrow u_{i,y}(B, q) = e^{iea^2 i_x B}$$

1) L-QCD in external (background) magnetic field.

Discretization details and numerical setup.

QCD with $N_f = 2$ mass-degenerate flavours: u and d quark.

$$q_u = +(2/3)|e| \quad q_d = -(1/3)|e|$$

Partition function for rooted staggered fermions:

$$Z = \int \mathcal{D}U \mathcal{P}[m, U, B, Q] = \int \mathcal{D}U e^{-S_G} \det M^{1/4}[m, B, q_u] \det M^{1/4}[m, B, q_d]$$

the staggered fermion matrix M in presence of the background is:

$$M_{i,j}[B, q] = \hat{m} \delta_{i,j} + \frac{1}{2} \sum_{\mu=1}^4 \eta_{i,\mu} (U'_{i,\mu}(B, q) \delta_{i,j-\hat{\mu}} - U'^{\dagger}_{i-\hat{\mu},\mu}(B, q) \delta_{i,j+\hat{\mu}})$$

where

$$U'_{i,\mu}(B, q) = u_{i,\mu}(B, q) \quad U_{i,\mu}$$

To have $\mathbf{B} = B\hat{z}$ we choose $A_{\mu}^{\text{EM}}(\mathbf{x}) = (0, xB, 0, 0)$ so that:

$$u_{i,\mu}(B, q) = 1 \text{ unless } \mu = y \rightarrow u_{i,y}(B, q) = e^{iea^2 i_x B}$$

1) L-QCD in external (background) magnetic field.

Discretization details and numerical setup.

QCD with $N_f = 2$ mass-degenerate flavours: u and d quark.

$$q_u = +(2/3)|e| \quad q_d = -(1/3)|e|$$

Partition function for rooted staggered fermions:

$$Z = \int \mathcal{D}U \mathcal{P}[m, U, B, Q] = \int \mathcal{D}U e^{-S_G} \det M^{1/4}[m, B, q_u] \det M^{1/4}[m, B, q_d]$$

the staggered fermion matrix M in presence of the background is:

$$M_{i,j}[B, q] = \hat{m} \delta_{i,j} + \frac{1}{2} \sum_{\mu=1}^4 \eta_{i,\mu} (U'_{i,\mu}(B, q) \delta_{i,j-\hat{\mu}} - U'^{\dagger}_{i-\hat{\mu},\mu}(B, q) \delta_{i,j+\hat{\mu}})$$

where

$$U'_{i,\mu}(B, q) = u_{i,\mu}(B, q) \ U_{i,\mu}$$

To have $\mathbf{B} = B\hat{z}$ we choose $A_{\mu}^{\text{EM}}(\mathbf{x}) = (0, xB, 0, 0)$ so that:

$$u_{i,\mu}(B, q) = 1 \text{ unless } \mu = y \rightarrow u_{i,y}(B, q) = e^{iea^2 i_x B}$$

1) L-QCD in external (background) magnetic field.

($|q|B$) is quantized. Why?

- We want a **uniform z-oriented** magnetic field.
- Periodic Space-B.C. : x-y plane is a **torus**

1) L-QCD in external (background) magnetic field.

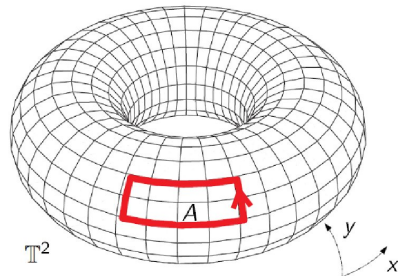
($|q|B$) is quantized. Why?

- We want a **uniform z-oriented** magnetic field.
- Periodic Space-B.C. : x-y plane is a **torus** → closed surface.

1) L-QCD in external (background) magnetic field.

($|q|B$) is quantized. Why?

- We want a **uniform z-oriented** magnetic field.
- Periodic Space-B.C. : x-y plane is a **torus** \rightarrow closed surface.



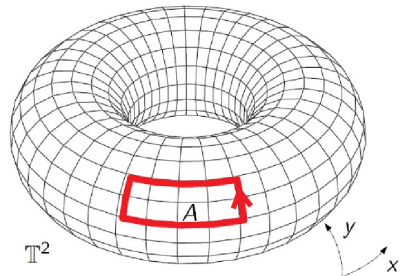
Effect: **quantization of ($|q|B$)**

$$q\Phi_A(B) = q\Phi_{T^2-A}(B) + 2\pi b$$

1) L-QCD in external (background) magnetic field.

($|q|B$) is quantized. Why?

- We want a **uniform z-oriented** magnetic field.
- Periodic Space-B.C. : x-y plane is a **torus** \rightarrow closed surface.



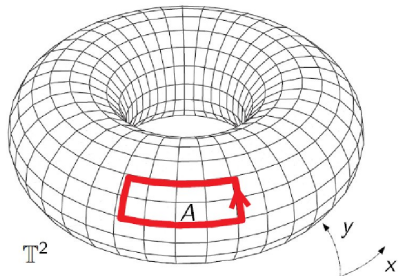
Effect: **quantization of ($|q|B$)**

$$qAB = q(A - l_x l_y)B + 2\pi b$$

1) L-QCD in external (background) magnetic field.

($|q|B$) is quantized. Why?

- We want a **uniform z-oriented** magnetic field.
- Periodic Space-B.C. : x-y plane is a **torus** \rightarrow closed surface.



Effect: **quantization of ($|q|B$)**

$$qAB = q(A - l_x l_y)B + 2\pi b$$

which implies

$$(qB) = \frac{2\pi b}{l_x l_y} = \frac{2\pi b}{a^2 L_x L_y}$$

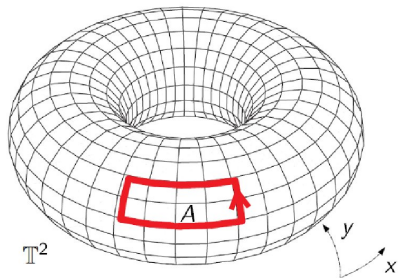
So that

$$u_{i,y} = e^{i \frac{2\pi b i_x}{L_x L_y}}$$

1) L-QCD in external (background) magnetic field.

($|q|B$) is quantized. Why?

- We want a **uniform z-oriented** magnetic field.
- Periodic Space-B.C. : x-y plane is a **torus** \rightarrow closed surface.



More details in [Al-Hashimi and Wiese; arXiv:0807.0630]

Effect: **quantization of ($|q|B$)**

$$qAB = q(A - I_x I_y)B + 2\pi b$$

which implies

$$(qB) = \frac{2\pi b}{I_x I_y} = \frac{2\pi b}{a^2 L_x L_y}$$

So that

$$u_{i,y} = e^{i \frac{2\pi b i x}{L_x L_y}}$$

1) L-QCD in external (background) magnetic field.

Algorithm: Rational Hybrid Monte Carlo (**RHMC**)

Adimensional parameters:

- lattice size $L_x = L_y = L_z = L_t = 16$
- beta gauge $\beta = 5.30$
- bare mass $\hat{m} = 0.01335$
- field quanta $b \in [0, L_x L_y] \equiv [0, 256]$

Dimensional parameters:

- lattice spacing $a \simeq 0.3 \text{ fm} \rightarrow (1/a \simeq 660 \text{ MeV})$
- temperature $T \simeq 40 \text{ MeV} \rightarrow \text{below } \chi \text{ and deconf. transitions.}$
- pion mass $m_\pi \simeq 200 \text{ MeV}$
- field range $(|e|B) \in (180 - 700 \text{ MeV})^2 \sim (10^{14} - 10^{15}) T$

Warning!

Because of 2π periodicity of the magnetic-phase and B inversion symmetry we naively expect:

- Observables $L_x L_y$ -periodicity in b
- Saturation effects

1) L-QCD in external (background) magnetic field.

Algorithm: Rational Hybrid Monte Carlo (**RHMC**)

Adimensional parameters:

- lattice size $L_x = L_y = L_z = L_t = 16$
- beta gauge $\beta = 5.30$
- bare mass $\hat{m} = 0.01335$
- field quanta $b \in [0, L_x L_y] \equiv [0, 256]$

Dimensional parameters:

- lattice spacing $a \simeq 0.3 \text{ fm} \rightarrow (1/a \simeq 660 \text{ MeV})$
- temperature $T \simeq 40 \text{ MeV} \rightarrow \text{below } \chi \text{ and deconf. transitions.}$
- pion mass $m_\pi \simeq 200 \text{ MeV}$
- field range $(|e|B) \in (180 - 700 \text{ MeV})^2 \sim (10^{14} - 10^{15}) T$

Warning!

Because of 2π periodicity of the magnetic-phase and B inversion symmetry we naively expect:

- Observables $L_x L_y$ -periodicity in b
- Saturation effects

1) L-QCD in external (background) magnetic field.

Algorithm: Rational Hybrid Monte Carlo (**RHMC**)

Adimensional parameters:

- lattice size $L_x = L_y = L_z = L_t = 16$
- beta gauge $\beta = 5.30$
- bare mass $\hat{m} = 0.01335$
- field quanta $b \in [0, L_x L_y] \equiv [0, 256]$

Dimensional parameters:

- lattice spacing $a \simeq 0.3 \text{ fm} \rightarrow (1/a \simeq 660 \text{ MeV})$
- temperature $T \simeq 40 \text{ MeV} \rightarrow \text{below } \chi \text{ and deconf. transitions.}$
- pion mass $m_\pi \simeq 200 \text{ MeV}$
- field range $(|e|B) \in (180 - 700 \text{ MeV})^2 \sim (10^{14} - 10^{15}) T$

Warning!

Because of 2π periodicity of the magnetic-phase and B inversion symmetry we naively expect:

- Observables $L_x L_y$ -periodicity in b
- Saturation effects

1) L-QCD in external (background) magnetic field.

Algorithm: Rational Hybrid Monte Carlo (**RHMC**)

Adimensional parameters:

- lattice size $L_x = L_y = L_z = L_t = 16$
- beta gauge $\beta = 5.30$
- bare mass $\hat{m} = 0.01335$
- field quanta $b \in [0, L_x L_y] \equiv [0, 256]$

Dimensional parameters:

- lattice spacing $a \simeq 0.3 \text{ fm} \rightarrow (1/a \simeq 660 \text{ MeV})$
- temperature $T \simeq 40 \text{ MeV} \rightarrow \text{below } \chi \text{ and deconf. transitions.}$
- pion mass $m_\pi \simeq 200 \text{ MeV}$
- field range $(|e|B) \in (180 - 700 \text{ MeV})^2 \sim (10^{14} - 10^{15}) T$

Warning!

Because of 2π periodicity of the magnetic-phase and B inversion symmetry we naively expect:

- Observables $L_x L_y$ -periodicity in b
- Saturation effects

2) Magnetic catalysis and chiral symmetry breaking.

Magnetic catalysis \equiv increase of χ -SB due to the magnetic field.

How does $\Sigma(B) = <\bar{\psi}\psi>$, the quark condensate, depends on B?

We have $N_f = 2$ flavours so

$$\Sigma(B) = <\bar{u}u> + <\bar{d}d> = \Sigma_u(B) + \Sigma_d(B).$$

Let's define their's relative increments: $r_{u/d}(B) = \frac{\Sigma_{u/d}(B) - \Sigma(0)}{\Sigma(0)}$.

2) Magnetic catalysis and chiral symmetry breaking.

Magnetic catalysis \equiv increase of χ -SB due to the magnetic field.

How does $\Sigma(B) = <\bar{\psi}\psi>$, the quark condensate, depends on B ?

We have $N_f = 2$ flavours so

$$\Sigma(B) = <\bar{u}u> + <\bar{d}d> = \Sigma_u(B) + \Sigma_d(B).$$

Let's define their's relative increments: $r_{u/d}(B) = \frac{\Sigma_{u/d}(B) - \Sigma(0)}{\Sigma(0)}$.

Residual renormalization effects on r :

- multiplicative due to additive mass dependent \rightarrow non-negligible
(order of 10%)
- residual B dependent \rightarrow negligible if $|e|B$ away from UV cutoff

2) Magnetic catalysis and chiral symmetry breaking.

Magnetic catalysis \equiv increase of χ -SB due to the magnetic field.

How does $\Sigma(B) = <\bar{\psi}\psi>$, the quark condensate, depends on B ?

We have $N_f = 2$ flavours so

$$\Sigma(B) = <\bar{u}u> + <\bar{d}d> = \Sigma_u(B) + \Sigma_d(B).$$

Let's define their's relative increments: $r_{u/d}(B) = \frac{\Sigma_{u/d}(B) - \Sigma(0)}{\Sigma(0)}$.

Since $q_u \neq q_d$ we expect $r_u \neq r_d$!

Many models predicts particular functional forms for $r(B)$.

What about full (L)QCD?

2) Magnetic catalysis and chiral symmetry breaking.

Contributions to magnetic catalysis.

In general one can try to compute:

$$\Sigma_j(m, m', B, B') = \int \mathcal{D}U \mathcal{P}[m', U, B'] \text{Tr}(M^{-1}[m, B, q_j])$$

2) Magnetic catalysis and chiral symmetry breaking.

Contributions to magnetic catalysis.

In general one can try to compute:

$$\Sigma_j(\textcolor{blue}{m}, m', \textcolor{blue}{B}, B') = \int \mathcal{D}U \mathcal{P}[m', U, B'] \textcolor{blue}{\text{Tr}}(M^{-1}[\textcolor{blue}{m}, B, q_j])$$

2) Magnetic catalysis and chiral symmetry breaking.

Contributions to magnetic catalysis.

In general one can try to compute:

$$\Sigma_j(m, \textcolor{blue}{m}', B, \textcolor{blue}{B}') = \int \mathcal{D}U \mathcal{P}[m', U, \textcolor{blue}{B}'] \text{Tr}(M^{-1}[m, B, q_j])$$

2) Magnetic catalysis and chiral symmetry breaking.

Contributions to magnetic catalysis.

- Valence contribution (or pseudo-quenched):

$$\Sigma_{u/d}^{\text{val}}(B) = \int \mathcal{D}U \mathcal{P}[m, U, 0] \text{Tr}(M^{-1}[m, B, q_j])$$

- Dynamical contribution:

$$\Sigma_{u/d}^{\text{dyn}}(B) = \int \mathcal{D}U \mathcal{P}[m, U, B] \text{Tr}(M^{-1}[m, 0, q_j])$$

- Total contribution:

$$\Sigma_{u/d}(B) = \int \mathcal{D}U \mathcal{P}[m, U, B] \text{Tr}(M^{-1}[m, B, q_j])$$

2) Magnetic catalysis and chiral symmetry breaking.

Contributions to magnetic catalysis.

- Valence contribution (or pseudo-quenched):

$$\Sigma_{u/d}^{\text{val}}(B) = \int \mathcal{D}U \mathcal{P}[m, U, 0] \text{Tr}(M^{-1}[m, B, q_j])$$

- Dynamical contribution:

$$\Sigma_{u/d}^{\text{dyn}}(B) = \int \mathcal{D}U \mathcal{P}[m, U, B] \text{Tr}(M^{-1}[m, 0, q_j])$$

- Total contribution:

$$\Sigma_{u/d}(B) = \int \mathcal{D}U \mathcal{P}[m, U, B] \text{Tr}(M^{-1}[m, B, q_j])$$

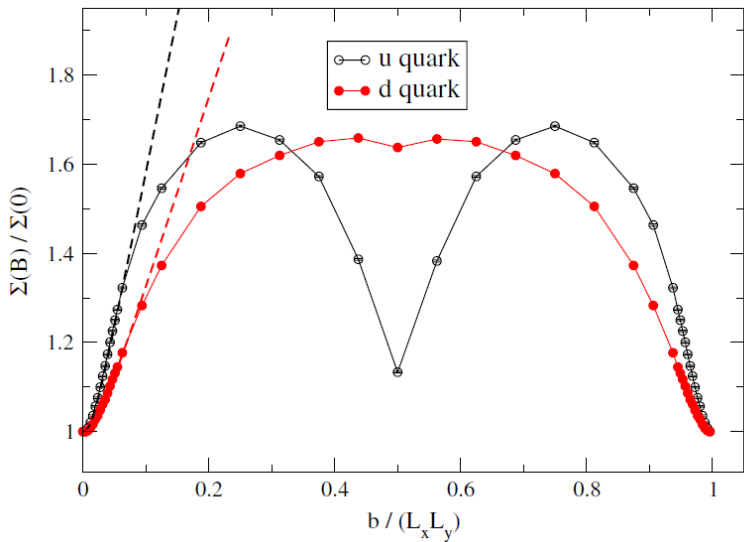
Assuming that the effects of B on \mathcal{P} and on the observable are **small perturbations**:

$$r_{u/d}(B) = r_{u/d}^{\text{val}}(B) + r_{u/d}^{\text{dyn}}(B) + \mathcal{O}(B^4)$$

3) Numerical results and other model comparisons.

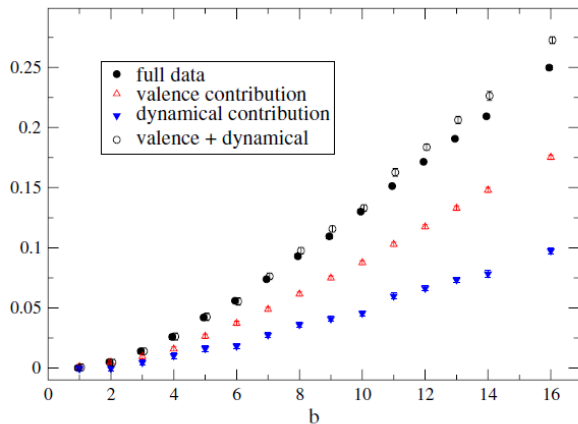
Periodicity and saturation effects.

[Phys.Rev. D 83, 114028 (2011)]



3) Numerical results and other model comparisons.

Valence and Dynamical contributions to catalysis.
[Phys.Rev. D 83, 114028 (2011)]



$$\bullet r(B) \simeq r^{\text{dyn}}(B) + r^{\text{val}}(B)$$

$$\bullet r^{\text{dyn}}(B) \simeq 0.4 \cdot r(B)$$

3) Numerical results and other model comparisons.

Some remarks about *val* and *dyn* contribution.

- **Additivity** of *val* and *dyn* to produce the total signal:
signature that the magnetic field B acts as a small perturbation.
- We are starting to see **deviation** when saturation effects
are significant and when $\sqrt{|e|B}$ approaches to the UV cutoff.
- Unquenching increases the signal ($\sim 40\%$ of the total).

$$r^{\text{val}}(B) \simeq 0.6 r(B) \quad \text{and} \quad r^{\text{dyn}}(B) \simeq 0.4 r(B)$$

3) Numerical results and other model comparisons.

Review of some model predictions.

- NJL model (et al.); [Klevansky and Lemmer; Phys.Rev. D 39, 3478 (1989)]
 $r(B) \propto (|e|B)^2$
- χ PT, $m_\pi = 0$; [Shushpanov and Smilga; Phys.Lett. B 402, 351 (1997)]
 $r(B) \propto (|e|B)$
- χ PT, $m_\pi \neq 0$; [Cohen et al.; Phys.Rev. C 76, 055201 (2007)]
 $r(B) \propto (|e|B) \cdot \mathcal{I}\left(\frac{m_\pi^2}{(|e|B)}\right)$
- quenched SU(2); [Buividovich et al.; Phys.Lett. B 682, 484 (2010)]
 $r(B) \propto (|e|B)$
- quenched SU(3); [Braguta et al.; arXiv:hep-lat/1011.3795]
 $r(B) \propto (|e|B)^\nu \quad \nu \sim 1.6$

3) Numerical results and other model comparisons.

Review of some model predictions.

- NJL model (et al.); [Klevansky and Lemmer; Phys.Rev. D 39, 3478 (1989)]
 $r(B) \propto (|e|B)^2 \rightarrow \text{OK up to } b=7 \quad (|e|B) \sim (480\text{MeV})^2$
- χ PT, $m_\pi = 0$; [Shushpanov and Smilga; Phys.Lett. B 402, 351 (1997)]
 $r(B) \propto (|e|B)$
- χ PT, $m_\pi \neq 0$; [Cohen et al.; Phys.Rev. C 76, 055201 (2007)]
 $r(B) \propto (|e|B) \cdot \mathcal{I}\left(\frac{m_\pi^2}{(|e|B)}\right)$
- quenched SU(2); [Buividovich et al.; Phys.Lett. B 682, 484 (2010)]
 $r(B) \propto (|e|B)$
- quenched SU(3); [Braguta et al.; arXiv:hep-lat/1011.3795]
 $r(B) \propto (|e|B)^\nu \quad \nu \sim 1.6$

3) Numerical results and other model comparisons.

Review of some model predictions.

- NJL model (et al.); [Klevansky and Lemmer; Phys.Rev. D 39, 3478 (1989)]
 $r(B) \propto (|e|B)^2$ → OK up to $b=7$ ($|e|B \sim (480\text{MeV})^2$)
- χ PT, $m_\pi = 0$; [Shushpanov and Smilga; Phys.Lett. B 402, 351 (1997)]
 $r(B) \propto (|e|B)$ → Never fits
- χ PT, $m_\pi \neq 0$; [Cohen et al.; Phys.Rev. C 76, 055201 (2007)]
 $r(B) \propto (|e|B) \cdot \mathcal{I}\left(\frac{m_\pi^2}{(|e|B)}\right)$
- quenched SU(2); [Buividovich et al.; Phys.Lett. B 682, 484 (2010)]
 $r(B) \propto (|e|B)$
- quenched SU(3); [Braguta et al.; arXiv:hep-lat/1011.3795]
 $r(B) \propto (|e|B)^\nu$ $\nu \sim 1.6$

3) Numerical results and other model comparisons.

Review of some model predictions.

- NJL model (et al.); [Klevansky and Lemmer; Phys.Rev. D 39, 3478 (1989)]
 $r(B) \propto (|e|B)^2$ → OK up to $b=7$ ($|e|B \sim (480\text{MeV})^2$)
- χ PT, $m_\pi = 0$; [Shushpanov and Smilga; Phys.Lett. B 402, 351 (1997)]
 $r(B) \propto (|e|B)$ → Never fits
- χ PT, $m_\pi \neq 0$; [Cohen et al.; Phys.Rev. C 76, 055201 (2007)]
 $r(B) \propto (|e|B) \cdot \mathcal{I}\left(\frac{m_\pi^2}{(|e|B)}\right)$ → OK up to $b=13$ ($|e|B \sim (650\text{MeV})^2$)
- quenched SU(2); [Buividovich et al.; Phys.Lett. B 682, 484 (2010)]
 $r(B) \propto (|e|B)$
- quenched SU(3); [Braguta et al.; arXiv:hep-lat/1011.3795]
 $r(B) \propto (|e|B)^\nu$ $\nu \sim 1.6$

3) Numerical results and other model comparisons.

Review of some model predictions.

- NJL model (et al.); [Klevansky and Lemmer; Phys.Rev. D 39, 3478 (1989)]
 $r(B) \propto (|e|B)^2$ → OK up to $b=7$ ($|e|B \sim (480\text{MeV})^2$)
- χ PT, $m_\pi = 0$; [Shushpanov and Smilga; Phys.Lett. B 402, 351 (1997)]
 $r(B) \propto (|e|B)$ → Never fits
- χ PT, $m_\pi \neq 0$; [Cohen et al.; Phys.Rev. C 76, 055201 (2007)]
 $r(B) \propto (|e|B) \cdot \mathcal{I}\left(\frac{m_\pi^2}{(|e|B)}\right)$ → OK up to $b=13$ ($|e|B \sim (650\text{MeV})^2$)
- quenched SU(2); [Buividovich et al.; Phys.Lett. B 682, 484 (2010)]
 $r(B) \propto (|e|B)$ → Never fits
- quenched SU(3); [Braguta et al.; arXiv:hep-lat/1011.3795]
 $r(B) \propto (|e|B)^\nu$ $\nu \sim 1.6$

3) Numerical results and other model comparisons.

Review of some model predictions.

- NJL model (et al.); [Klevansky and Lemmer; Phys.Rev. D 39, 3478 (1989)]
 $r(B) \propto (|e|B)^2$ → OK up to b=7 ($|e|B \sim (480\text{MeV})^2$)
- χ PT, $m_\pi = 0$; [Shushpanov and Smilga; Phys.Lett. B 402, 351 (1997)]
 $r(B) \propto (|e|B)$ → Never fits
- χ PT, $m_\pi \neq 0$; [Cohen et al.; Phys.Rev. C 76, 055201 (2007)]
 $r(B) \propto (|e|B) \cdot \mathcal{I}\left(\frac{m_\pi^2}{(|e|B)}\right)$ → OK up to b=13 ($|e|B \sim (650\text{MeV})^2$)
- quenched SU(2); [Buividovich et al.; Phys.Lett. B 682, 484 (2010)]
 $r(B) \propto (|e|B)$ → Never fits
- quenched SU(3); [Braguta et al.; arXiv:hep-lat/1011.3795]
 $r(B) \propto (|e|B)^\nu$ $\nu \sim 1.6 \rightarrow$ OK up to b=8 and $\nu \sim 2$ ($|e|B \sim (510\text{MeV})^2$)

3) Numerical results and other model comparisons.

Parameter Fit with 1-loop χ PT.

$$r(B) = \frac{\log(2)(|e|B)}{16\pi^2 F_\pi^2} \mathcal{I}\left(\frac{m_\pi^2}{(|e|B)}\right)$$

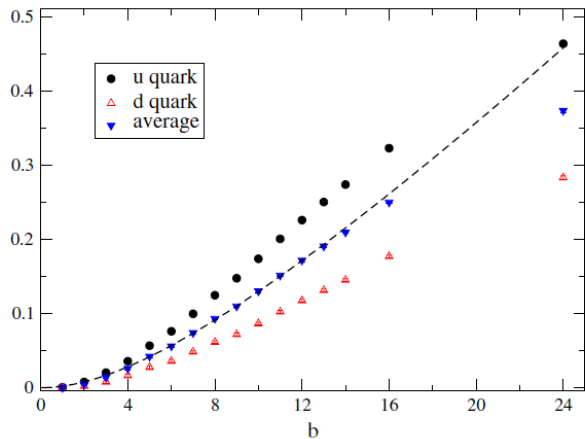
where

$$\mathcal{I}(y) = \frac{1}{\log(2)} \left(\log(2\pi) + y \log\left(\frac{y}{2}\right) - y - 2 \log\left(\Gamma\left(\frac{1+y}{2}\right)\right) \right)$$

b_{\min}	b_{\max}	χ^2/ndf	m_π (MeV)	F_π (MeV)
1	8	0.63	457(59)	54.7(5.6)
1	9	0.93	392(39)	61.7(4.2)
1	10	0.89	374(27)	63.8(2.9)
1	11	0.80	369(20)	64.3(2.1)
1	12	0.79	359(15)	65.6(1.6)
1	13	0.97	344(14)	67.2(1.4)
1	14	1.40	328(14)	69.1(1.4)
1	16	1.92	310(13)	71.1(1.3)

3) Numerical results and other model comparisons.

Parameter Fit with 1-loop χ PT.



4) Conclusions.

Studying $N_f = 2$ (L)QCD with a magnetic background:

- we studied magnetic catalysis, i.e. the increase of chiral symmetry breaking induced by the magnetic field.
- we have explicitly shown periodicity and saturation effects.
- dynamical fermions provide about 40% of the total contribution to magnetic catalysis.
- the best fitting functional form: 1-loop χ PT with $m_\pi \neq 0$.